JOURNAL OF MATERIALS SCIENCE 31 (1996) 6631–6636

An algorithm for simulating the isothermal hysteresis in the stress–strain laws of shape memory alloys

R. D. SPIES*
Department of Mathematics, Iowa State University, 400 Carver Hall, Ames, IA 50011, USA

An algorithm for simulating the hysteresis in the stress–strain laws of Shape Memory Alloys (SMAs) is presented. The algorithm stores the sequences of dominant input extrema of the strain history allowing points in the interior of the outer-most loops to be reached, in agreement with the behaviour observed experimentally. A numerical example is shown.

1. Introduction

The hysteresis phenomenon which characterizes the stress–strain relations of pseudoelastic materials is due mainly to the existence of local and/or global memories. This can be easily seen by the fact that a particular load can produce different deformations depending on the initial state which, in terms, depends on the strain history (see, for instance [1], p. 78, Fig. 2.14). In a series of articles [2–6], Falk introduced a model that captures several important characteristics of shape memory alloys (SMAs). Falk's model consists essentially of defining a non-convex thermodynamic potential, Ψ, in the form of a Hemholtz free energy density, which is considered to be a function of macroscopic strain, ε, and the absolute temperature, θ. The function, Ψ, is chosen in such a way that it satisfies all the underlying hypotheses of the Landau theory of phase transitions [7] and, at the same time, it reproduces the experimentally observed behaviour of SMAs. A simple form of this function, Ψ, is found to be the so-called Landau–Devonshire potential

$$\Psi(\varepsilon, \theta) = \Psi_0(\theta) + \alpha_2(\theta - \theta_1)\varepsilon^2 - \alpha_4\varepsilon^4 + \alpha^6\varepsilon^6 \quad (1)$$

where $\Psi_0(\theta)$ is some smooth function of the temperature, α_2, α_4, α_6 are positive non physical constants and θ_1 is a critical temperature, all depending on the material being considered. To avoid this dependence on the material, dimensionless quantities are introduced by means of the following normalization.

$$f = \frac{\alpha_6^2}{\alpha_4^3}\Psi \quad (2a)$$

$$e = \left(\frac{\alpha_6}{\alpha_4}\right)^{1/2}\varepsilon \quad (2b)$$

$$t = \frac{\alpha_6\alpha_2}{\alpha_4^2}(\theta - \theta_1) - \frac{1}{4} \quad (2c)$$

$$f_0 = \frac{\alpha_6^2}{\alpha_4^3}\Psi_0(\theta) \quad (2d)$$

The normalized free energy is then independent of any particular parameter and takes the form

$$f(e, t) = f_0(t) + \left(t - \frac{1}{4}\right)e^2 - e^4 + e^6 \quad (3)$$

(see Fig. 1). Using this representation for the free energy, several thermodynamic functions are derived. The stress–strain relations, for example, are given by

$$\sigma = \frac{\partial f}{\partial e} = 2\left(t + \frac{1}{4}\right)e - 4e^3 + 6e^5 \quad (4)$$

(see Fig. 2). Falk's idea has already been incorporated into several dynamic models that require an explicit form for the free-energy potential [8–12]. However, it is not difficult to realize that the potential (Equation 1) does not completely capture the behaviour of SMAs. We observe, for example, that the same stress–strain relation is obtained, independently of whether the material is under loading or unloading. In particular, for intermediate temperatures, in the non-monotonic region, Equation 4 predicts states on one of the diagonals of the hysteresis loop which is observed experimentally in an SMA material. Furthermore, there are materials for which certain particular loading–unloading regimes result in "nested" hysteresis loops in the corresponding stress–strain relations. In fact, isothermal, uniaxial stretching experiments under controlled deformation performed in CuZnAl alloys [13] (see Fig. 3) have shown that it is possible for any state within the outermost loops to be reached. These states can be both the result of unloading after partial yield, due to strain hardening or the result of reloading after a partial recovery. In order to capture this type of behaviour, a different approach is needed.

* *Permanent address*: Instituto de Desarrollo Technológico para la Industria Química INTEC, Programa Especial de Matemática Aplicada PEMA, CONICET, Universidad Nacional del Litoral, Güemes 3450, (3000) Santa Fe, Argentina.

0022–2461

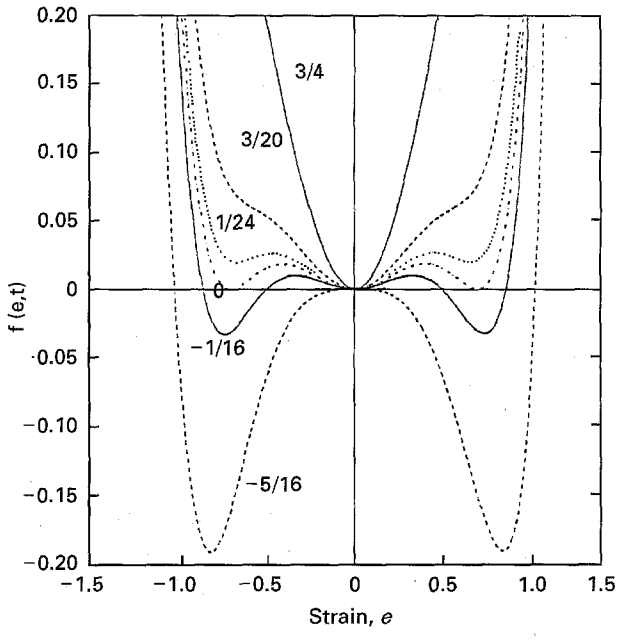

Figure 1 The normalized Landau–Devonshire potential.

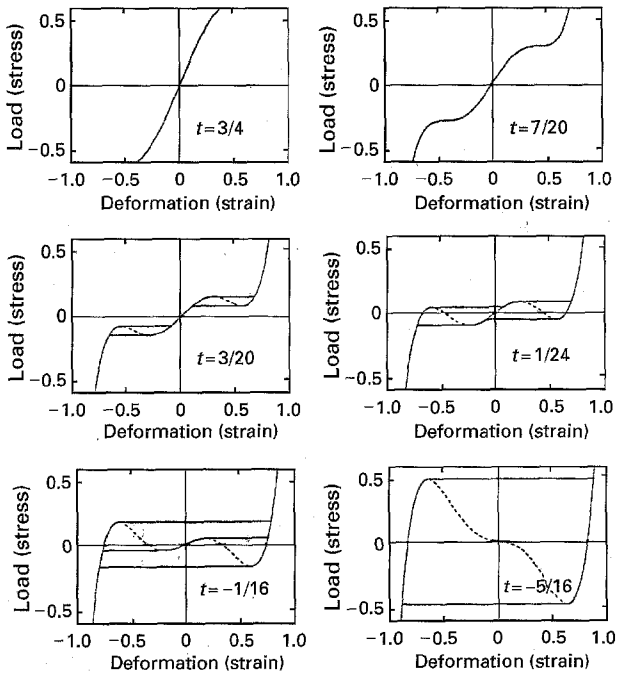

Figure 2 Stress–strain laws obtained with the Landau–Devonshire potential.

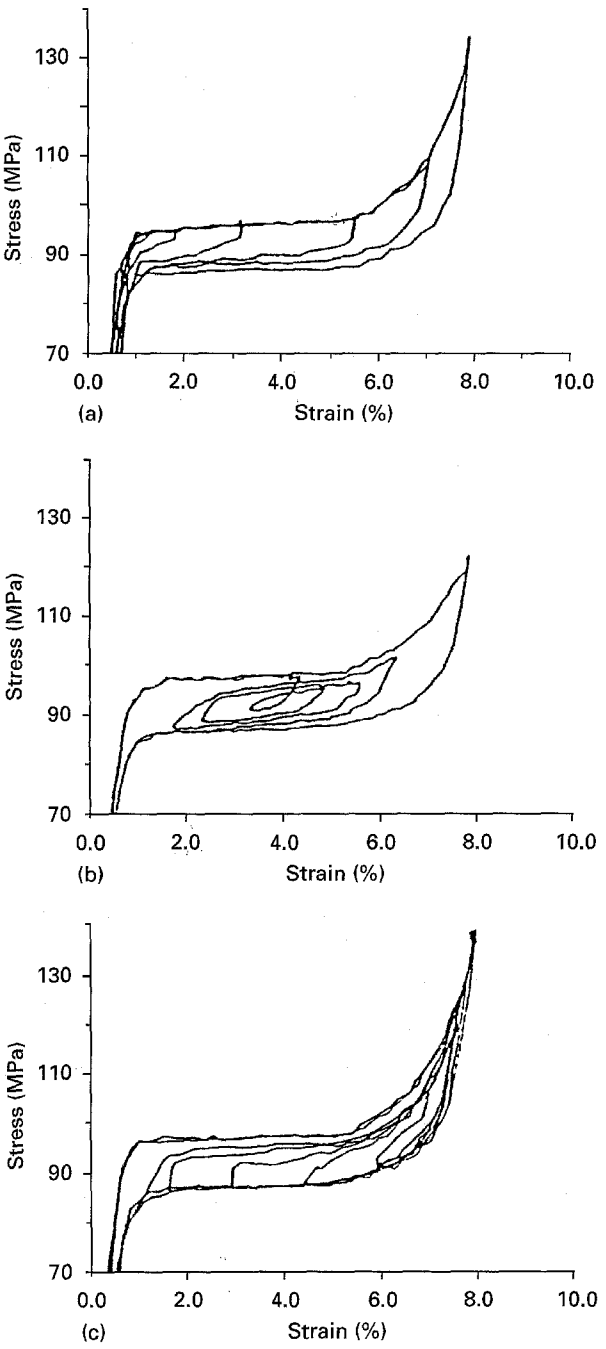

Figure 3 Isothermal stress–strain relations obtained from uniaxial stretching experiments under controlled deformation performed in CuZnAl alloys. (a) Unloading after partial yield; (b) interior "nested" hysteresis loops; (c) reloading after partial recovery [13].

2. The model

The approach followed in this work consists essentially of parametrizing the first-order transition curves and introducing suitable parameters in order to take into account local memories and phase fractions.

For a fixed temperature θ, we assume that the outermost loop is completely characterized by the eight values ε_i, σ_i, $1 \leqslant i \leqslant 4$, with $0 \leqslant \varepsilon_1 < \varepsilon_2 < \varepsilon_3 < \varepsilon_4$, $0 \leqslant \sigma_1 \leqslant \sigma_2 < \sigma_3 \leqslant \sigma_4$, as shown in Fig. 4. These eight critical values will strongly depend on the temperature, θ. Note that σ_3 estimates the modulus of elasticity in tension corresponding to the temperature θ.

Let $\mathscr{U} = \{\Gamma_\beta^U(\cdot)\}_{0 \leqslant \beta \leqslant 1}$ be the family of curves parametrized by β shown in Fig. 5 (the superscript U stands for unloading). The curve $\Gamma_\beta^U(\varepsilon)$ is defined explicitly below. Let

$$\varepsilon_\beta^{0,U} \doteq \beta\varepsilon_1 + (1-\beta)\varepsilon_2; \quad \sigma_\beta^{0,U} \doteq \beta\sigma_1 + (1-\beta)\sigma_3 \tag{5a}$$

$$\varepsilon_\beta^{1,U} \doteq \beta\varepsilon_3 + (1-\beta)\varepsilon_2; \quad \sigma_\beta^{1,U} \doteq \beta\sigma_2 + (1-\beta)\sigma_3 \tag{5b}$$

$$\varepsilon_\beta^{2,U} \doteq \beta\varepsilon_4 + (1-\beta)\varepsilon_2; \quad \sigma_\beta^{2,U} \doteq \beta\sigma_4 + (1-\beta)\sigma_3 \tag{5c}$$

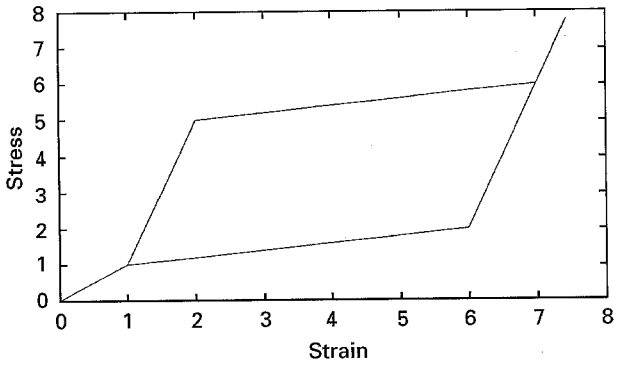

Figure 4 Characterization of the outermost loops by using the eight critical values ε_i, σ_i, $i = 1, \ldots, 4$.

and define $\Gamma_\beta^U(\varepsilon)$ by

$$\Gamma_\beta^U(\varepsilon) \doteq$$

$$\begin{cases} \dfrac{\sigma_1}{\varepsilon_1}\varepsilon & \text{for } 0 \leqslant \varepsilon < \varepsilon_1 \\ \sigma_1 + \dfrac{\sigma_\beta^{0,U} - \sigma_1}{\varepsilon_\beta^{0,U} - \varepsilon_1}(\varepsilon - \varepsilon_1) & \text{for } \varepsilon_1 \leqslant \varepsilon < \varepsilon_\beta^{0,U} \\ \sigma_\beta^{0,U} + \dfrac{\sigma_\beta^{1,U} - \sigma_\beta^{0,U}}{\varepsilon_\beta^{1,U} - \varepsilon_\beta^{0,U}}(\varepsilon - \varepsilon_\beta^{0,U}) & \text{for } \varepsilon_\beta^{0,U} \leqslant \varepsilon < \varepsilon_\beta^{1,U} \\ \sigma_\beta^{1,U} + \dfrac{\sigma_\beta^{2,U} - \sigma_\beta^{1,U}}{\varepsilon_\beta^{2,U} - \varepsilon_\beta^{1,U}}(\varepsilon - \varepsilon_\beta^{1,U}) & \text{for } \varepsilon_\beta^{1,U} \leqslant \varepsilon < \varepsilon_\beta^{2,U} \\ \sigma_\beta^{2,U} + \dfrac{\sigma_4 - \sigma_\beta^{2,U}}{\varepsilon_4 - \varepsilon_\beta^{2,U}}(\varepsilon - \varepsilon_\beta^{2,U}) & \text{for } \varepsilon_\beta^{2,U} \leqslant \varepsilon < \varepsilon_4 \\ \sigma_2 + \dfrac{\sigma_4 - \sigma_2}{\varepsilon_4 - \varepsilon_3}(\varepsilon - \varepsilon_3) & \text{for } \varepsilon \geqslant \varepsilon_4 \end{cases} \tag{6}$$

Similarly, let $\mathscr{L} = \{\Gamma_\beta^L(\cdot)\}_{0 \leqslant \beta \leqslant 1}$ be the family of curves parametrized by β shown in Fig. 6 (the superscript L stands for loading). The curve $\Gamma_\beta^L(\varepsilon)$ is defined by the parameters

$$\varepsilon_\beta^{0,L} \doteq \beta\varepsilon_3 + (1-\beta)\varepsilon_1; \quad \sigma_\beta^{0,L} \doteq \beta\sigma_2 + (1-\beta)\sigma_1 \tag{7a}$$

$$\varepsilon_\beta^{1,L} \doteq \beta\varepsilon_3 + (1-\beta)\varepsilon_2; \quad \sigma_\beta^{1,L} \doteq \beta\sigma_2 + (1-\beta)\sigma_3 \tag{7b}$$

$$\varepsilon_\beta^{2,L} \doteq \beta\varepsilon_3 + (1-\beta)\varepsilon_4; \quad \sigma_\beta^{2,L} \doteq \beta\sigma_2 + (1-\beta)\sigma_4 \tag{7c}$$

and

$$\Gamma_\beta^L(\varepsilon) \doteq$$

$$\begin{cases} \dfrac{\sigma_1}{\varepsilon_1}\varepsilon & \text{for } 0 \leqslant \varepsilon < \varepsilon_1 \\ \sigma_1 + \dfrac{\sigma_\beta^{0,L} - \sigma_1}{\varepsilon_\beta^{0,L} - \varepsilon_1}(\varepsilon - \varepsilon_1) & \text{for } \varepsilon_1 \leqslant \varepsilon < \varepsilon_\beta^{0,L} \\ \sigma_\beta^{0,L} + \dfrac{\sigma_\beta^{1,L} - \sigma_\beta^{0,L}}{\varepsilon_\beta^{1,L} - \varepsilon_\beta^{0,L}}(\varepsilon - \varepsilon_\beta^{0,L}) & \text{for } \varepsilon_\beta^{0,L} \leqslant \varepsilon < \varepsilon_\beta^{1,L} \\ \sigma_\beta^{1,L} + \dfrac{\sigma_\beta^{2,L} - \sigma_\beta^{1,L}}{\varepsilon_\beta^{2,L} - \varepsilon_\beta^{1,L}}(\varepsilon - \varepsilon_\beta^{1,L}) & \text{for } \varepsilon_\beta^{1,L} \leqslant \varepsilon < \varepsilon_\beta^{2,L} \\ \sigma_2 + \dfrac{\sigma_4 - \sigma_2}{\varepsilon_4 - \varepsilon_3}(\varepsilon - \varepsilon_3) & \text{for } \varepsilon \geqslant \varepsilon_\beta^{2,L} \end{cases} \tag{8}$$

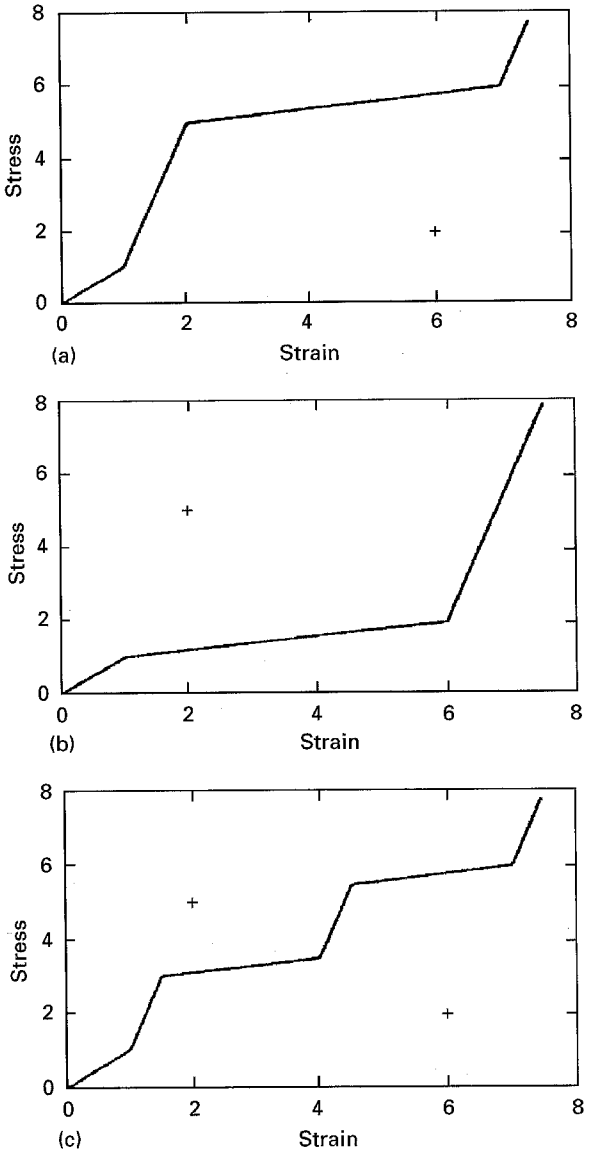

Figure 5 $\Gamma_\beta^U(\varepsilon)$: (a) $\beta = 0$; (b) $\beta = 1$; (c) $0 < \beta < 1$.

Observe that $\Gamma_0^L(\cdot) \equiv \Gamma_0^U(\cdot)$, $\Gamma_1^L(\cdot) \equiv \Gamma_1^U(\cdot)$, $\varepsilon_\beta^{1,L} = \varepsilon_\beta^{1,U}$ and $\varepsilon_\beta^{1,L} = \sigma_\beta^{1,U}$.

We add dynamics to the model as follows. Let $\Gamma_{\beta_0}^{w_0}$ be our initial curve, $0 \leqslant \beta_0 \leqslant 1$, $w_0 = \mathrm{U}$ or L. Let $\beta(t=0) = \beta_0$, $w(t=0) = w_0$ and $(\varepsilon_0, \sigma_0)$ a point on $\Gamma_{\beta_0}^{w_0}$ (i.e. $\sigma_0 = \Gamma_{\beta_0}^{w_0}(\varepsilon_0)$). Let $\varepsilon(t)$, $0 \leqslant t \leqslant T$ be our strain input, where T denotes a certain prescribed final time. We assume that ε is a continuous function of t on the interval $[0, T]$ and satisfies the initial condition $\varepsilon(0) = \varepsilon_0$.

The points $(\varepsilon(t), \sigma(t))$ will remain on the curve $\Gamma_{\beta_0}^{w_0}$ until the next relative extremum of $\varepsilon(t)$ occurs. In general, $\beta(t)$ and $w(t)$ will remain constant between any two consecutive relative extrema of $\varepsilon(t)$. Let t^* be the minimum positive time such that t^* is a relative extremum of $\varepsilon(t)$. One now updates w and β as follows.

First case: Maximum. Suppose that $\varepsilon(t)$ has a relative maximum at $t = t^*$. This means that $w_0 = \mathrm{L}$ and the points $(\varepsilon(t), \sigma(t))$ are on $\Gamma_{\beta_0}^L$ for $0 \leqslant t < t^*$. Now define $w(t^*)$ to be U. To update β one must find β^* such that

$$\begin{cases} \Gamma_{\beta_0}^L(\varepsilon(t^*)) = \Gamma_{\beta^*}^U(\varepsilon(t^*)) \\ 0 \leqslant \beta^* \leqslant 1 \end{cases} \tag{9}$$

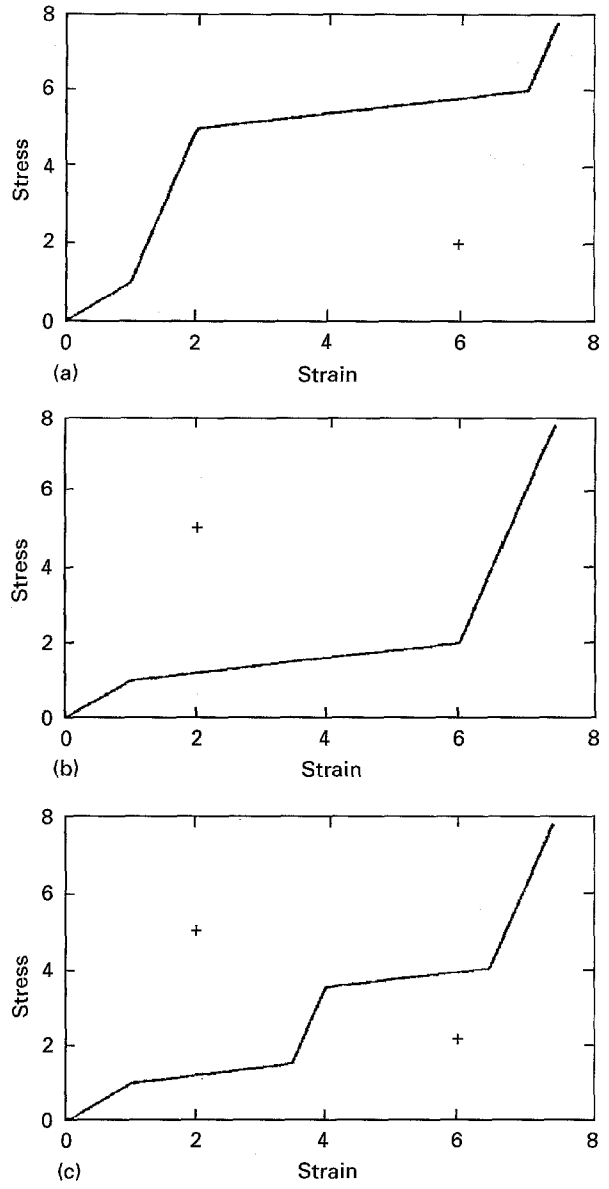

Figure 6 $\Gamma^{L}_{\beta}(\varepsilon)$: (a) $\beta = 0$; (b) $\beta = 1$; (c) $0 < \beta < 1$.

The appropriate value of β^* is given by the following algorithm:

(1) if $\varepsilon(t^*) \geqslant \varepsilon^{2,L}_{\beta_0}$ or $\varepsilon(t^*) \leqslant \varepsilon^{0,L}_{\beta_0}$ then $\beta^* = 1$;

(2) if $\varepsilon^{1,L}_{\beta_0} < \varepsilon(t^*) < \varepsilon^{2,L}_{\beta_0}$, then

$$\beta^* = \frac{\varepsilon(t^*) - \varepsilon^{0,U}_{\beta_0}}{\varepsilon^{2,L}_{\beta_0} - \varepsilon^{0,U}_{\beta_0}} \tag{10}$$

(3) finally, if $\varepsilon^{0,L}_{\beta_0} < \varepsilon(t^*) < \varepsilon^{1,L}_{\beta_0}$, then

$$\beta^* = \frac{\varepsilon(t^*) - \varepsilon^{2,U}_{\beta_0}}{\varepsilon^{0,L}_{\beta_0} - \varepsilon^{2,U}_{\beta_0}} \tag{11}$$

In cases 2 and 3, the solution β^* is unique. Once w and β have been updated, $w(t) = U$, $\beta(t) = \beta^*$ and $\sigma(t) = \Gamma^{w(t)}_{\beta(t)}[\varepsilon(t)] = \Gamma^{U}_{\beta^*}[\varepsilon(t)]$ for $t^* \leqslant t < t^{**}$ where t^{**} is the next relative minimum of $\varepsilon(t)$.

Second case: minimum. Suppose that $\varepsilon(t)$ has a relative minimum at $t = t^*$. This means that $w_0 = U$ and the points $(\varepsilon(t), \sigma(t))$ are on $\Gamma^{U}_{\beta_0}$ for $0 \leqslant t < t^*$. Then, w is updated by changing it from U to L. To update β one needs to find β^* such that

$$\begin{cases} \Gamma^{U}_{\beta_0}(\varepsilon(t^*)) = \Gamma^{L}_{\beta_*}(\varepsilon(t^*)) \\ 0 \leqslant \beta^* \leqslant 1 \end{cases} \tag{12}$$

Again, the appropriate value of β^* is given by the following algorithm

(1) if $\varepsilon(t^*) \geqslant \varepsilon^{2,U}_{\beta_0}$ or $\varepsilon(t^*) \leqslant \varepsilon^{0,U}_{\beta_0}$ then $\beta^* = 0$;

(2) if $\varepsilon^{1,U}_{\beta_0} < \varepsilon(t^*) < \varepsilon^{2,U}_{\beta_0}$, then

$$\beta^* = \frac{\varepsilon(t^*) - \varepsilon^{2,U}_{\beta_0}}{\varepsilon^{0,L}_{\beta_0} - \varepsilon^{2,U}_{\beta_0}} \tag{13}$$

(3) finally, if $\varepsilon^{0,U}_{\beta_0} < \varepsilon(t^*) \leqslant \varepsilon^{1,U}_{\beta_0}$ then

$$\beta^* = \frac{\varepsilon(t^*) - \varepsilon^{0,U}_{\beta_0}}{\varepsilon^{2,L}_{\beta_0} - \varepsilon^{0,U}_{\beta_0}} \tag{14}$$

Again, in cases 2 and 3 the solution β^* is unique. Once w and β have been updated, $w(t) = L$, $\beta(t) = \beta^*$ and $\sigma(t) = \Gamma^{w(t)}_{\beta(t)}(\varepsilon(t)) = \Gamma^{L}_{\beta^*}(\varepsilon(t))$ for $t^* \leqslant t < t^{**}$ where t^{**} is the next relative maximum of $\varepsilon(t)$. At $t = t^{**}$, the above procedure is repeated to update w and β.

An analysis of the dynamics imposed on this model reveals that for $0 < \beta < 1$ the definition of $\Gamma^{L}_{\beta}(\varepsilon)$ on the interval $\varepsilon_1 < \varepsilon < \varepsilon^{0,L}_{\beta}$ is superfluous. In fact, that part of the curve will never be followed under loading and its definition is given only for the sake of completeness.

By assuming a linear relation across the yield lines, the (martensite) phase fraction $f_{M^+}(\varepsilon(t), \beta(t), w(t))$ can be computed as follows

$$f_{M^+}[\varepsilon(t), \beta(t), w(t)] \doteq \begin{cases} f_U[\varepsilon(t), \beta(t)] & \text{if } w(t) = U \\ f_L[\varepsilon(t), \beta(t)] & \text{if } w(t) = L \end{cases} \tag{15}$$

where

$$f_U(\varepsilon, \beta) \doteq \begin{cases} 0 & \text{for } \varepsilon \leqslant \varepsilon^{0,U}_{\beta} \\ \dfrac{(\varepsilon^{2,U}_{\beta} - \varepsilon_2)(\varepsilon - \varepsilon^{0,U}_{\beta})}{(\varepsilon_4 - \varepsilon_2)(\varepsilon^{1,U}_{\beta} - \varepsilon^{0,U}_{\beta})} & \text{for } \varepsilon^{0,U}_{\beta} < \varepsilon < \varepsilon^{1,U}_{\beta} \\ \dfrac{\varepsilon^{2,U}_{\beta} - \varepsilon_2}{\varepsilon_4 - \varepsilon_2} & \text{for } \varepsilon^{1,U}_{\beta} \leqslant \varepsilon \leqslant \varepsilon^{2,U}_{\beta} \\ \dfrac{\varepsilon - \varepsilon_2}{\varepsilon_4 - \varepsilon_2} & \text{for } \varepsilon^{2,U}_{\beta} < \varepsilon < \varepsilon_4 \\ 1 & \text{for } \varepsilon \geqslant \varepsilon_4 \end{cases} \tag{16}$$

and

$$f_L(\varepsilon, \beta) \doteq \begin{cases} 0 & \text{for } \varepsilon \leqslant \varepsilon_1 \\ \dfrac{(\varepsilon^{2,U}_{\beta} - \varepsilon_2)(\varepsilon - \varepsilon_1)}{(\varepsilon_4 - \varepsilon_2)(\varepsilon^{0,L}_{\beta} - \varepsilon_1)} & \text{for } \varepsilon_1 < \varepsilon < \varepsilon^{0,L}_{\beta} \\ \dfrac{\varepsilon^{2,U}_{\beta} - \varepsilon_2}{\varepsilon_4 - \varepsilon_2} & \text{for } \varepsilon^{0,L}_{\beta} \leqslant \varepsilon \leqslant \varepsilon^{1,L}_{\beta} \\ \dfrac{\varepsilon^{2,U}_{\beta} - \varepsilon_2}{\varepsilon_4 - \varepsilon_2} + \dfrac{(\varepsilon_4 - \varepsilon^{2,U}_{\beta})(\varepsilon - \varepsilon^{1,L}_{\beta})}{(\varepsilon_4 - \varepsilon_2)(\varepsilon^{2,L}_{\beta} - \varepsilon^{1,L}_{\beta})} & \text{or } \varepsilon^{1,L}_{\beta} < \varepsilon < \varepsilon^{2,L}_{\beta} \\ 1 & \text{for } \varepsilon \geqslant \varepsilon^{2,L}_{\beta} \end{cases} \tag{17}$$

3. A numerical example

Consider the particular case in which $\varepsilon_1 = 1$, $\varepsilon_2 = 2$, $\varepsilon_3 = 6$, $\varepsilon_4 = 7$, $\sigma_1 = 1$, $\sigma_2 = 2$, $\sigma_3 = 5$ and $\sigma_4 = 6$. Let $\varepsilon(t)$, for $0 \leqslant t \leqslant 7$, be as shown in Fig. 7.

The stress–strain curve obtained with the dynamics described above corresponding to the input $\varepsilon(t)$ is shown in Fig. 8. Note how the alternating series of dominant input extrema is stored by the model and results in "nested" hysteresis loops. Fig. 9 shows a graphical representation of the (martensite) phase fraction f_{M^+} as a function of the time t. The behaviour of $\beta(t)$ is shown in Fig. 10. Fig. 11 shows the martensite fraction f_{M^+} as a function of the strain ε, parametrized by the time t. Note here that for $\varepsilon_1 < \varepsilon < \varepsilon_4$, the strain does not determine uniquely the phase fraction. In fact, for those values of ε, a whole interval of possible phase fractions is obtained. Finally, Fig. 12 shows a comparison of the stresses obtained with the standard Landau–Devonshire model and the model described here. Compare these profiles with that of Fig. 3b.

The stress–strain relations incorporate the "strain history" through the dynamics described above. This model possesses three properties which are characteristic of the Preisach models of hysteresis [14], namely the wiping-out and congruency properties and the fading-memory property. The first one states that only the alternating series of dominant input extrema are stored by the model, while all other input extrema are wiped out. The congruency property consists of the fact that all minor hysteresis loops corresponding to back-and-forth variations of inputs between the same two consecutive extremum values, are congruent. For these reasons, this representation can be viewed as a simplified Preisach model.

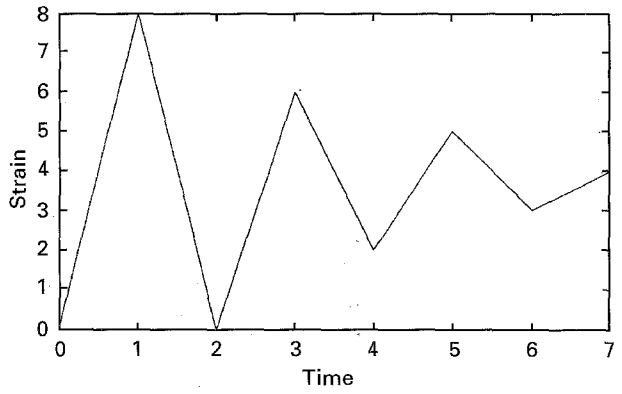

Figure 7 Strain input $\varepsilon(t)$.

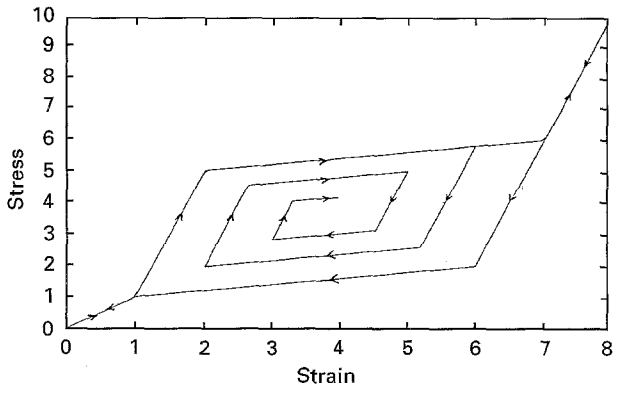

Figure 8 Stress (output) $\sigma(t)$ as a function of the strain (input) $\varepsilon(t)$, parametrized by the time t.

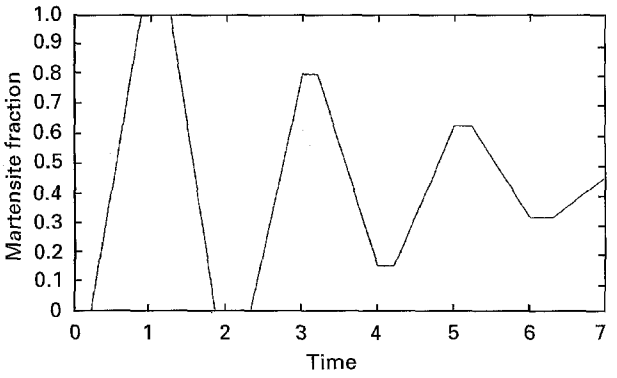

Figure 9 Martensite fraction f_{M^+} as a function of time t.

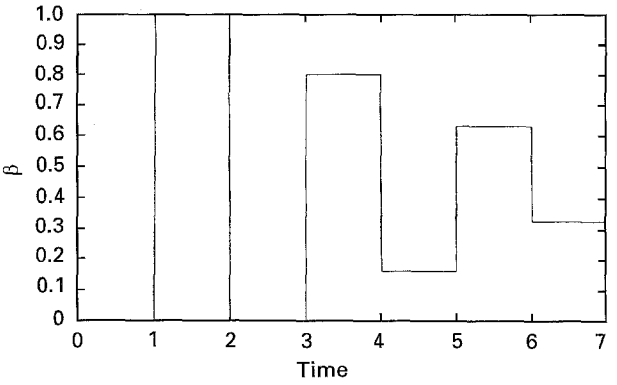

Figure 10 The parameter β as a function of time t.

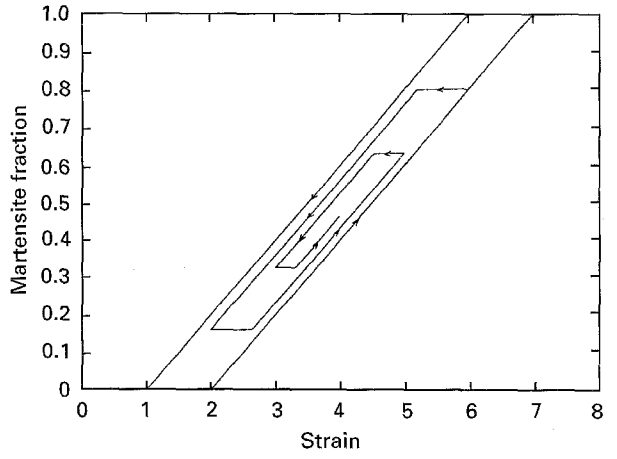

Figure 11 The (martensite) f_{M^+} phase fraction as a function of the strain ε parametrized by the time t.

4. Conclusion

An algorithm has been presented to simulate the hysteresis in the stress–strain laws of shape memory alloys. At each time step, t, the algorithm stores the sequences of dominant input extrema of the strain (input). Decreasing sequences of maxima and increasing sequences of minima in the strain result in nested hysteresis loops, in accordance with results observed

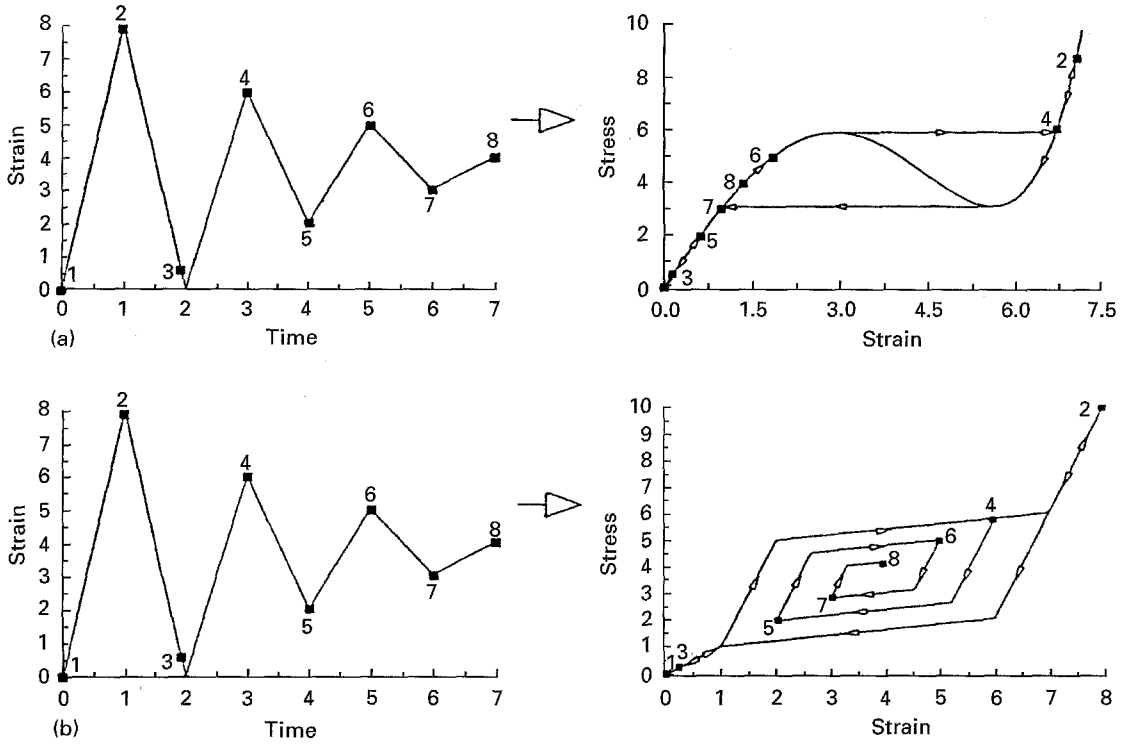

Figure 12 Comparison between the stresses obtained with (a) the standard Landau–Devonshire model and (b) the new model for the same strain input.

experimentally. A comparison with the standard Landau–Devonshire potential is provided.

The sharp edges in the stress–strain output obtained with this algorithm are a direct result of the linear relations used for the first-order transition curves. Obviously, the use of piecewise quadratic or cubic polynomials would not only avoid these sharp edges but would also provide a closer fitting to the experimental results. The fact that we have used linear relations was made merely for simplicity reasons in order to illustrate the usefulness of the algorithm.

Acknowledgements

The work of the author was supported in part by the Argentinean National Council for Scientific and Technical Research CONICET and by the US Air Force Office of Scientific Research (AFOSR) under grant F49620-92-J-0078 and by the Institute for Mathematics and Its Applications of the University of Minnesota with funds provided by the Office of Naval Research (ONR) through grant N/N0014-93-1-0027 and by the National Science Foundation (NSF) through grant NSF/DMS-9023978 while the author was a postdoctoral fellow at the Institute for Mathematics and Its Applications of the University of Minnesota.

References

1. H. FUNAKUBO, "Shape Memory Alloys", Precision Machinery and Robotics, Vol. 1, Translated from the Japanese by J. B. Kennedy (Gordon and Breach Science Publishers, New York, 1987).
2. F. FALK, *J. Phys. Coll. C4, Supp. 12* **43** (1982) C4 203.
3. *Idem, Acta Metall.* **28** 1773.
4. *Idem, Arch. Mech.* **35** (1983) 63.
5. *Idem, Int. J. Eng. Sci.* **27** (1989) 277.
6. *Idem, ZAMM* **60** (1980) T 118.
7. *Idem, J. Phys. Coll. C4 Suppl. 12* **43** (1982) C4 3.
8. J. A. BURNS and R. D. SPIES, in "Proceedings of the ADPA/AIAA/ASME/SPIE Conference on Active Materials and Adaptive Structures", Alexandria, VA (1991) IOP Publishing, 1992, pp. 207–10.
9. *Idem*, in "Proceedings of the 30th IEEE Conference on Decision and Control", Brighton, UK (1991) (IEEE, 1991) pp. 2334–9.
10. *Idem, J. Intelligent Mater. Syst. Struct.* **5** (3), (1994) 321.
11. R. D. SPIES, *J. Math. Anal. Applic.* **190** (1995) 58.
12. *Idem, J. Smart Struct. Mater.* **3** (1994) 459.
13. I. MULLER and H. XU, *Acta Metall.* **39** (1991) 263.
14. I. D. MAYERGOYZ, "Mathematical Models of Hysteresis" (Springer, New York, 1991).

Received 5 October 1994
and accepted 1 December 1995